24th IMEKO TC4 International Symposium
22nd International Workshop on ADC and DAC Modelling and Testing
IMEKO TC-4 2020
Palermo, Italy, September 14-16, 2020

Compressive sampling–based vector signal analysis for distributed spectrum monitoring

Luca De Vito, Francesco Picariello, Sergio Rapuano, Ioan Tudosa

Department of Engineering, Unversity of Sannio, Benevento, Italy
e-mail: {devito, fpicariello, rapuano, ioan.tudosa}@unisannio.it

***Abstract* – This paper investigates the application of Compressive Sampling (CS) for the realization of a Vector Signal Analyzer (VSA) node for distributed spectrum monitoring. Herein, the non-uniform sampling approach is proposed for the signal acquisition section of the node, under the assumption of sparsity of the acquired signal in the frequency domain. A simulation analysis has been conducted to assess several figures of merit, characterizing the performance in the frequency and modulation domains. The obtained results demonstrate that the CS could reduce the amount of acquired samples by a factor greater than 10, while still complying with the accuracy required by spectrum monitoring applications.**

I. INTRODUCTION

Radio Frequency (RF) spectrum monitoring represents an activity of primary importance, both in the civil and military field [1]. In the military field, monitoring is essential for application of Electronic Warfare or Electronic Support Measure, where it is necessary to sense, intercept, identify, localize, record and/or analyze RF energy sources, with the aim of recognizing an immediate threat or of organizing a long-term operative planning. In the civil field, spectrum monitoring is necessary to guarantee the security of sites and infrastructures that are critical for the homeland security, such as airports, power plants, embassies. Moreover, with the increase of the number and of the band occupation of the telecommunication systems, the radio spectrum monitoring became a necessary activity to verify the correct usage of the spectrum and the simultaneous coexistence of multiple communication systems [2].

RF spectrum monitoring is currently carried out by means of Vector Signal Analyzers (VSA). A VSA consists of a Radio Frequency (RF) receiver named front-end (i.e. containing amplifiers, mixers, and filters), and a data acquisition back-end, containing an Analog-to-Digital Converter (ADC), and digital signal processing unit (e.g. Field Programmable Gate Array (FPGA), Digital Signal Processor (DSP), Central Processing Unit (CPU), and Graphics Processing Unit (GPU)) [3], [4]. Traditionally, the VSA utilizes a down-conversion stage for the desired signal bandwidth to obtain a translation of it to a fixed frequency (i.e. Intermediate Frequency, IF). Thereafter, the obtained IF analog signal is sampled by the ADC. Thus, a stream of time domain samples is obtained, which can be used for various domain analyses. If the spectrum analysis is desired, the acquired time domain samples are processed to obtain the frequency domain spectrum of the observed signal by means of the Fast Fourier Transform (FFT), [4]. Besides FFT, in today's communication systems, the most used figure of merit for the accuracy evaluation of the digital modulation is the Error Vector Magnitude (EVM) (i.e. which contains both amplitude and phase errors). The EVM reports the gain imbalance of the in-phase (I) and quadrature (Q) signal components, the I-Q phase imbalance, and the phase noise [3], [5], [6].

In last years, with the increase of wireless transmitters and the wider use of higher frequencies in the GHz range, the classic approach of having single spectrum monitoring stations is no longer effective. Instead, a distributed network of sensing nodes should be deployed. However, the large data rate that must be sent from the distributed nodes to the control center limits the bandwidth that can be actually monitored.

Compressive Sampling (CS) has been proposed in the scientific literature for sampling signals that are sparse in a specific domain, such that they can be reconstructed without a significant quality loss [7].

In literature, the potential benefits of CS for VSA have been already demonstrated in [8], where a CS-based preprocessor has been proposed for modulation analysis. Moreover, it has been demonstrated in [9] and [10] that CS–based signal acquisition is suitable for RF emitter localization. This paper aims to evaluate the applicability of CS to realize VSA sensing nodes for distributed spectrum monitoring. In this case, CS is not only applied to modulation analysis, however it is used in the VSA sensing node, as shown in Fig. 1a, to reduce the amount of samples that are acquired downstream of the mixer and the ADC and that are sent to the data concentrator node (Fig. 1b), where the waveform is reconstructed and the required analysis is performed (time, frequency, modulation or code domain).

After the Introduction, the paper is structured as follows. In Section II, the proposed architecture of the proposed VSA sensing node, utilizing a digital non-uniform sampling based CS signal processing is presented. A brief overview of the adopted CS approach is mathematically

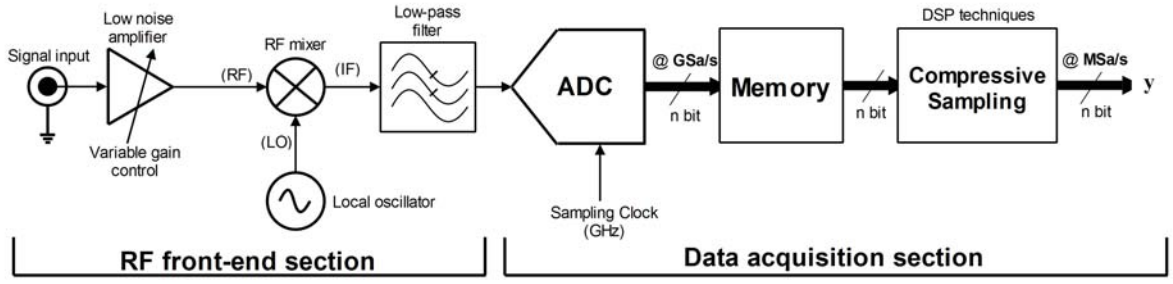

(a) Spectrum monitoring node

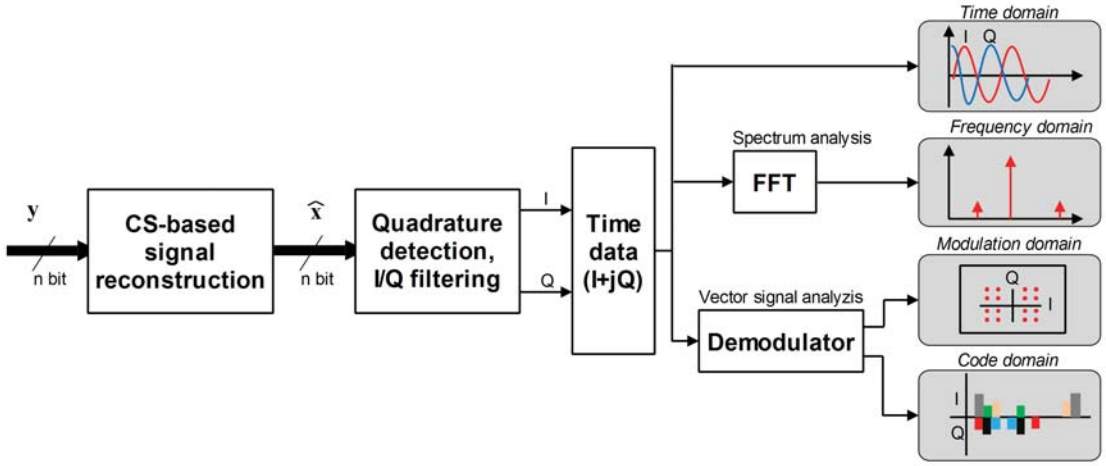

(b) Data concentrator node

Fig. 1. Block scheme of the proposed distributed spectrum monitoring system: (a) VSA sensing node, and (b) data concentrator node.

modelled and described. In Section III, the simulation strategy, the evaluated figures of merits, and the obtained numerical results are presented. Several conclusions and future work are drawn in the last Section of the paper.

II. THE PROPOSED ARCHITECTURE

In Fig. 1a, the architecture of the proposed VSA sensing node for RF spectrum monitoring is depicted. It is divided into two main parts, the RF front-end section and the data acquisition section. The former consists of: (i) a low noise amplifier having a variable gain, which allows adapting the input signal to the mixer RF input port, (ii) the RF mixer, which performs the downconversion of the incoming RF signal by mixing it with the Local Oscillator (LO) sinewave signal, and (iii) the low-pass filter, having a cutting frequency at maximum half of the sampling clock frequency of the ADC, thus filtering out the IF signal output delivered by the RF mixer. The latter section comprises: (i) the ADC, working at the sampling clock according to the Nyquist criterion for the considered signal bandwidth, and (ii) a buffering memory for local storage of the acquired samples, and (iii) a signal processing device which performs the CS process on the acquired samples and provides a compressed version of them.

Being the number of samples acquired by the ADC equal to N and the number of compressed samples equal to M, the Compression Ratio (CR) is defined as $CR = N/M$. The M compressed samples, which represent the elements of the output vector $\mathbf{y}$, are obtained by Non–Uniform Sampling (NUS). In detail, by considering $\mathbf{x}$, the vector of N samples acquired by the ADC at Nyquist rate, $\mathbf{y}$ is obtained by randomly selecting M elements of $\mathbf{x}$. This operation is modeled as follows:

$$\mathbf{y} = \mathbf{\Phi} \cdot \mathbf{x} \tag{1}$$

where, $\mathbf{\Phi}$ is a $M \times N$ matrix evaluated from the identity matrix $\mathbf{I}_N$ by taking the rows corresponding to the indexes of the selected elements of $\mathbf{x}$.

The compressed samples are sent to the data concen-

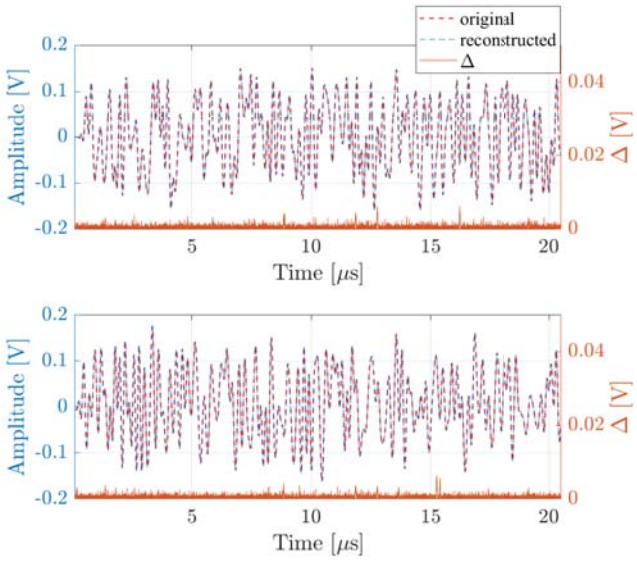

Fig. 2. The reconstructed I and Q signal components in the time domain for $CR = 10$.

trator node, which performs the signal reconstruction and shows to the user the reconstructed signal in several domains: (i) time domain, (ii) frequency domain, (iii) modulation domain, and (iv) code domain. The data processing chain performed by the data concentrator node is depicted in Fig. 1b. At the beginning, the CS reconstruction is performed to obtain an estimation of the original waveform $\mathbf{x}$. CS is based on the assumption that the input signal is sparse in a transform domain, i.e. its representation in such domain is a vector with few elements.

In this paper, sparsity in the Fourier domain is considered. Furthermore, in order to guarantee the reconstruction from the compressed samples, it is necessary that the sensing matrix $\mathbf{\Phi}$ presents a low coherence with the dictionary matrix (i.e. Discrete Fourier Transform (DFT) matrix), $\mathbf{\Psi}$, where the coherence is defined as:

$$\mu(\mathbf{\Phi}, \mathbf{\Psi}) = \sqrt{N} \cdot \max_{i,j} \frac{\boldsymbol{\phi}_i^T \boldsymbol{\psi}_j}{\|\boldsymbol{\phi}_i\|_2 \|\boldsymbol{\psi}_j\|_2}, \tag{2}$$

with $\boldsymbol{\phi}_i^T$ the i–th row of $\mathbf{\Phi}$,$\boldsymbol{\psi}_j$ the j–th column of $\mathbf{\Psi}$, and $\|\cdot\|_2$ indicating the ℓ_2 norm. The signal reconstruction is performed on the compressed vector, $\mathbf{y}$ stored in the memory by solving the following minimization problem:

$$\widehat{\boldsymbol{\alpha}} = \arg\min_{\boldsymbol{\alpha}} \|\boldsymbol{\alpha}\|_1, \ s.t. \ \mathbf{y} = \mathbf{\Phi}\mathbf{\Psi} \cdot \boldsymbol{\alpha} \tag{3}$$

where, $\|\cdot\|_1$ indicates the ℓ_1 norm operator, and $\boldsymbol{\alpha}$ is the $N \times 1$ vector of the DFT coefficients representing $\mathbf{x}$ in the Fourier domain. For solving (3), the Orthogonal Matching Pursuit (OMP) algorithm has been adopted [11].

Once the $\boldsymbol{\alpha}$ Fourier coefficients have been estimated, they can be directly shown versus the frequency, in the case a frequency domain analysis is required. For further analyses, the time domain signal is first obtained by:

$$\widehat{\mathbf{x}} = \mathbf{\Psi}\widehat{\boldsymbol{\alpha}} \tag{4}$$

Then, the I and Q components are obtained by means of a quadrature digital down-conversion. In the time domain analysis, the I and Q signals against acquisition time are shown to the user (see Fig. 2). In Fig. 2, the obtained I and Q components of the reconstructed signal (i.e. 16-QAM) from $CR = 10$ are compared with the original ones. It is possible to observe that the reconstructed signal (red lines) well-approximates the original one (blue lines). For performing analyses in the modulation domain, according to the estimated I and Q signals and by knowing the parameters of the raised-cosine filter used for generating the I and Q signals (i.e. roll-off factor and number of coefficients), the I and Q symbols in the complex plane are extrapolated.

In Fig. 3, the results obtained from the reconstructed signals according to 4-QAM, 16-QAM, and 64-QAM modulations are reported. For all the obtained results, the input signals are considered without additive noise and the CR of the CS is 10. From the obtained results, it is obtained that by increasing the number of symbols and by keeping the same $CR = 10$, the variability of the recognized I/Q components seems to increase. For the code domain analysis, each I/Q component is converted into its binary version according to the type of modulation (e.g. QAM, QPSK).

III. SIMULATION ANALYSIS

A MATLAB simulator has been developed for assessing the performance of the proposed VSA sensing node against CR. In particular, figures of merit have been evaluated according to the domains of analysis (see Fig. 1b): (i) time domain, (ii) frequency domain, (iii) modulation domain, and (iv) code domain. For the simulations, the mixer performs an ideal multiplication between the RF input signal and the LO, the low-pass filter has been implemented with a 100 taps length Finite Impulse Response (FIR) filter having a cut frequency of 500 MHz. The ADC works at 1 GSa/s with a resolution of 16-bit. The full scale of the ADC has been chosen according to the amplitude of the signal at the input of the ADC, so that its entire dynamics is exploited. Furthermore, for all the tests, the input signal has a carrier frequency of 2 GHz with a modulated signal having a roll-off factor of 0.2, and it has been considered without additive noise.

The considered modulation scheme is a Quadrature Amplitude Modulation (QAM) having a symbol rate of 10 MSymbol/s and a number of symbols ranging from 4 up to 64. For the sake of simplicity of the simulation tests, synchronous demodulation is considered, thus, the errors due to the recovery of the carrier frequency and the symbol rate are absent.

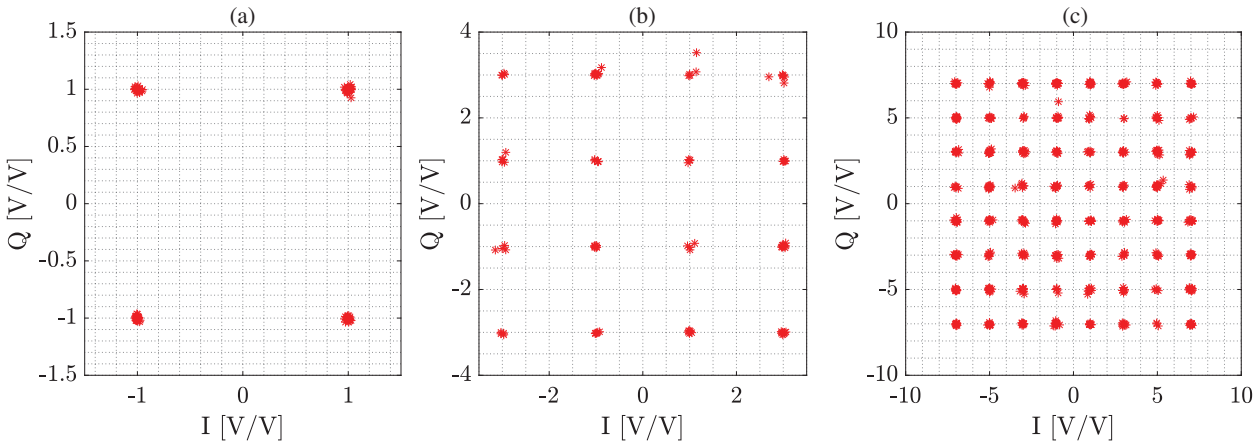

Fig. 3. Estimated I and Q symbols in the modulation domain for a $CR = 10$, for the a) 4-QAM, b) 16-QAM, c) 64-QAM modulation schemes.

A. Simulation strategy

For assessing the performance of the CS-based VSA sensing node in the time domain, the Root Mean Square Errors $RMSE$ for the I and Q signals, $RMSE(I)$ and $RMSE(Q)$, have been estimated according to the formula:

$$RMSE(l) = \frac{1}{N}\sqrt{\sum_{n=0}^{N-1}\left(\widehat{x(n)}_l - x(n)_l\right)^2} \tag{5}$$

where $l = I, Q$, $\widehat{x(n)}_I$ and $\widehat{x(n)}_Q$ are the reconstructed I and Q components, respectively, and $x(n)_I$ and $x(n)_Q$ are the I and Q components of the input signal.

In case of frequency domain analysis, the adopted figure of merit is the Spurious-Free Dynamic Range ($SFDR$). It has been assessed by considering, at the input of the VSA sensing node, a signal that is the sum of several sinewaves working at different frequencies according to the considered sparsity level $\frac{N_{bins}}{N/2}$, where N_{bins} is the number of considered sinewaves ranging from 16 to 250, and $N = 5000$.

In particular, if all the considered N_{bins} frequencies are correctly reconstructed, the $SFDR$ is given by:

$$SFDR = |\widehat{\alpha}|_{min,dB} - |\widehat{\alpha}|_{ext,dB} \tag{6}$$

where, $|\widehat{\alpha}|_{min,dB}$ is the minimum magnitude in dB among the N_{bins} signal coefficients, and $|\widehat{\alpha}|_{ext,dB}$ is the maximum magnitude in dB of the set of the remaining $N - N_{bins}$ estimated coefficients.

For assessing the performance in the modulation domain two figures of merit have been evaluated: (i) the Error Vector magnitude (EVM), and (ii) the Modulation Error Ratio (MER). The EVM is defined as follows:

$$EVM = \frac{\sqrt{\sum_{n=1}^{N_{sym}}\left(\widehat{I}(n) - I(n)\right)^2 + \left(\widehat{Q}(n) - Q(n)\right)^2}}{\sqrt{\sum_{n=1}^{N_{sym}} I(n)^2 + Q(n)^2}} \cdot 100 \tag{7}$$

where, $I(n)$ and $Q(n)$ with $n = 1, \ldots, N_{sym}$ are the I and Q symbols of the input signal, and $\widehat{I}(n)$ and $\widehat{Q}(n)$ are the estimated I and Q symbols.

The MER has been evaluated as follows:

$$MER = 10 \cdot log_{10}\left[\frac{\sum_{n=1}^{N_{sym}} I(n)^2 + Q(n)^2}{\sum_{n=1}^{N_{sym}}\left(\widehat{I}(n) - I(n)\right)^2 + \left(\widehat{Q}(n) - Q(n)\right)^2}\right] \tag{8}$$

The performance in the code domain has been assessed by evaluating the Symbol Error Rate SER. It is defined as the ratio between the number of symbols not correctly decoded and the total number of symbols.

B. Simulation results

For the assessment of the $RMSE(I)$ and $RMSE(Q)$ against compression ratio CR, Monte Carlo analyses have been performed on 100 trials by considering 4-QAM, 16-QAM, 32-QAM, and 64-QAM modulations. In Fig. 4, the average values of $RMSE(I)$ and $RMSE(Q)$ obtained for the 100 trials are reported for the considered CR values ranging from 10 up to 50 with a step of 10. As it was expected the $RMSE$ values increase with the compression ratio. Furthermore, by increasing the number of symbols for the QAM modulation the $RMSE$s increase. The amplitude of the input signal is 1 V and the $RMSE$ is lower than the 1 % of the amplitude for CRs up to 30 for 4-QAM, 16-QAM, and 32-QAM, and up to 20 for 64-QAM.

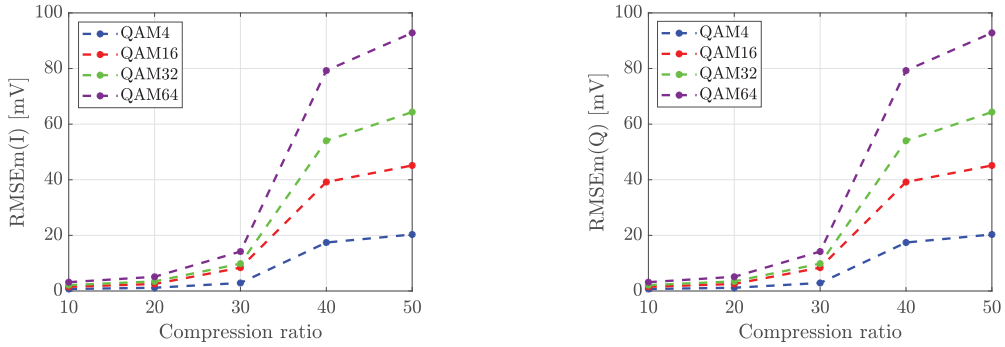

Fig. 4. Mean of RMSE (I/Q) vs. CR for 4-QAM, 16-QAM, 32-QAM, and 64-QAM modulations.

Monte Carlo analyses have been performed on 100 trials for assessing the $SFDR$ against sparsity level for several compression ratios CR from 10 up to 50 with a step of 10. The average values of the obtained $SFDR$ values for the 100 trials are shown in Fig. 5. At a given CR, the $SFDR$ decreases with the sparsity level (i.e., which is defined as the ratio between the number of frequency bins of the input signal and $N/2$). For all the CRs, the $SFDR$ values at the sparsity level of 0.1 are not provided because, due to the low sparsity of the input signal, it is not possible to reconstruct it from the compressed samples. Furthermore, by increasing the CR, the $SFDR$ values drastically decrease. For example, in case of $CR = 50$, the $SFDR$ is around 5 dB for the sparsity level of 0.012 and the signal is not correctly reconstructed at highest sparsity levels.

The averages of the EVM and the MER values, obtained from 100 Monte Carlo trials at several CRs and for the 4-QAM, 16-QAM, 32-QAM, and 64-QAM modulations, are depicted in Fig. 6 and Fig. 7, respectively. Both EVM and MER do not significantly change with the type of modulation. Of course, the EVM increases with the CR while the MER decreases. However, for achieving an EVM value lower than the 20 %, which corresponds to a MER value higher than 20 dB, the CR has to be lower than 30.

The SER values for the CRs of 10, 20, 30, 40, and 50 and by considering the 4-QAM, 16-QAM, 32-QAM, and 64-QAM modulations are depicted in Fig. 8. From the obtained results, it can be seen that the SER increases with the CR. For the CR of 10, in case of 4-QAM and 16-QAM, all the symbols are correctly reconstructed, thus the obtained SER is zero. By considering, an acceptable value of SER in the order of 10^{-4}, for 32-QAM and 64-QAM, a maximum CR of 20 can be used, for 16-QAM a maximum CR of 25 is obtained, and for 4-QAM, it can be increased up to 30.

IV. CONCLUSIONS AND FUTURE WORK

In this paper, the applicability of compressive sampling for the data rate reduction in VSA sensing nodes for distributed RF spectrum monitoring applications was investigated. The node architecture, exploiting signal reconstruction from a non-uniform CS samples was mathematically described. The obtained simulation results demonstrate that the adoption of CS for the implementation of distributed spectrum monitoring nodes is feasible. As a remark regarding the architecture of the VSA sensing node, described in Fig. 1a, it can be stated that the adoption of a such CS-based measurement method into Software

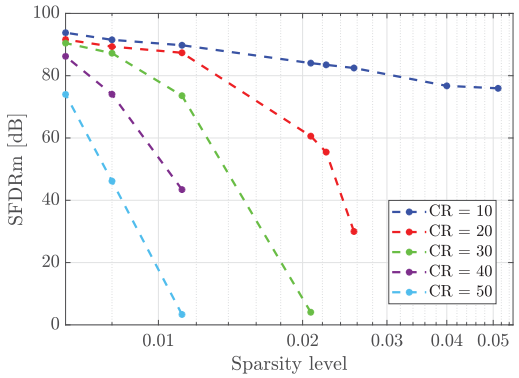

Fig. 5. Average SFDR vs. sparsity level for CR values ranging from 10 up to 50 with a step of 10.

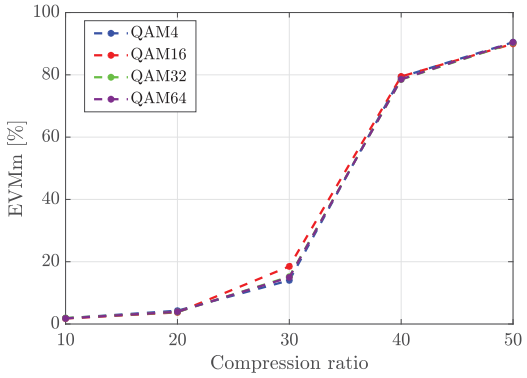

Fig. 6. Average EVM vs. CR for 4-QAM, 16-QAM, 32-QAM, and 64-QAM modulations.

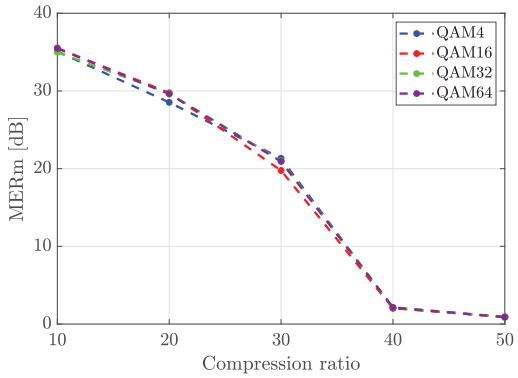

Fig. 7. Average MER vs. CR for 4*-QAM,* 16*-QAM,* 32*-QAM, and* 64*-QAM modulations.*

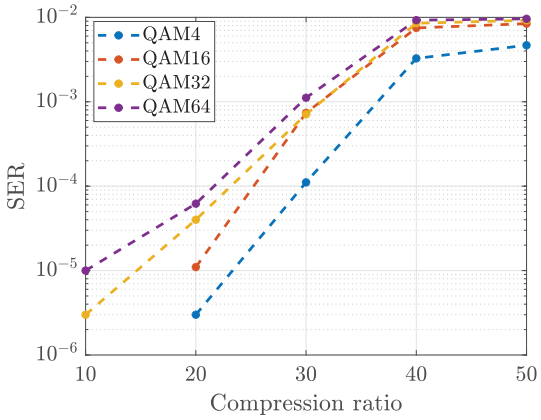

Fig. 8. SER vs. CR for 4*-QAM,* 16*-QAM,* 32*-QAM, and* 64*-QAM modulations.*

Defined Radio (SDR) apparatuses for signal compression, will not require adding extra hardware components. This will allow to deploy SDR sensors for very wideband RF vector signal analysis at remote stations by processing the compressed samples as in Fig. 1b.

Future work will be directed to: (i) develop a hardware prototype for the VSA sensing node, implementing the proposed architecture, (ii) experimental assess the implemented prototype, and (iii) further extend the research investigation for different sampling schemes, which can be adopted into CS–based VSA architectures.

ACKNOWLEDGMENT

The paper has been supported by the zSpectrum - *Compressed Spectrum for Radio Monitoring and Emission Localization* project, funded by the National Programme for Military Research PNRM n. a2018.008.

REFERENCES

[1] P. Daponte, L. De Vito, F. Picariello, S. Rapuano, and I. Tudosa, "Compressed Sensing technologies and challenges for aerospace and defense RF source localization", in *Proc. of 5th IEEE International Workshop on Metrology for AeroSpace (MetroAeroSpace)*, 20-22 June 2018, Roma, Italy, pp. 634–639.

[2] P. Daponte, L. De Vito, S. Rapuano, and I. Tudosa, "Analog-to-Information Converters in the wideband RF measurement for aerospace applications: current situation and perspectives", *IEEE Instrumentation Measurement Magazine*, vol. 20, No. 1, pp. 20–28, 2017.

[3] Keysight Technologies, *Vector signal analysis basics*, Application notes.

[4] Rohde & Schwarz, *Implementation of real-time spectrum analysis*, White paper.

[5] L. De Vito, S. Rapuano, and G. Truglia, "An improved method for classification and metrological characterization of disturbances on QAM signals", *IEEE Transactions on Instrumentation and Measurement*, vol. 55, No. 1, pp. 26–34, Feb. 2006.

[6] E. Balestrieri, L. De Vito, S. Rapuano, and D. Slepička, "Estimating the uncertainty in the frequency domain characterization of digitizing waveform recorders", *IEEE Trans. on Instrum. and Meas.*, vol. 61, No. 6, pp. 1613–1624, Jun. 2012.

[7] P. Daponte, L. De Vito, F. Picariello, S. Rapuano, and I. Tudosa, "Assessment of Analog-to-Information Converters based on non-uniform sampling for spectrum analysis", in *Proc. of IEEE Instrum. and Meas. Tech. Conf. (I2MTC)*, 14-17 May 2018, Houston, TX, pp. 1–6.

[8] C. Narduzzi and G. Frigo, "Characterization of a compressive sensing preprocessor for vector signal analysis", *IEEE Transactions on Instrumentation and Measurement*, vol. 65, No. 6, pp. 1319–1330, Jun. 2016.

[9] E. Balestrieri, L. De Vito, F. Picariello, and I. Tudosa, "A method exploiting compressive sampling for localization of radio frequency emitters", *IEEE Trans. on Instrumentation and Measurement*, vol. 69, No. 5, pp. 2325–2334, May 2020.

[10] E. Balestrieri, L. De Vito, F. Picariello, S. Rapuano, and I. Tudosa, "A TDoA-based measurement method for RF emitters localization by exploiting wideband Compressive Sampling", in *Proc. of IEEE Instrum. and Meas. Tech. Conf. (I2MTC)*, 25-28 May 2020, Dubrovnik, Croatia, pp. 1–6.

[11] J. A. Tropp and A. C. Gilbert, "Signal recovery from random measurements via orthogonal matching pursuit", *IEEE Transactions on Information Theory*, vol. 53, No. 12, pp. 4655–4666, Dec. 2007.